Heating of Jupiter's upper atmosphere above the Great Red Spot

Article

Accepted Version

Heating of Jupiter's upper atmosphere above the Great Red Spot

J. O'Donoghue[1], L. Moore[1], T.S. Stallard[2], H. Melin[2]
[1]Center for Space Physics, Boston University, Boston 02215, USA.
[2]Dept. of Physics & Astronomy, University of Leicester, Leicester, LE1 7RH, UK.

Measured upper-atmospheric, mid-to-low latitude temperatures of the giant planets are hundreds of degrees warmer than models based on solar heating alone can explain[1-4]. Modelling studies, focused on additional sources of heating, have been unable to resolve this significant model-data discrepancy. Equatorward transport of energy from the hot auroral regions was expected to heat low latitude regions; instead, models have demonstrated that auroral energy is trapped at high latitudes, a consequence of the strong Coriolis forces on these rapidly rotating planets[3-5]. Wave heating, driven from below, represents another potential source of upper-atmospheric heating, though initial calculations have proven inconclusive at Jupiter, largely due to a lack of observational constraints on wave parameters[6,7]. Here we report that the upper atmosphere above Jupiter's Great Red Spot - the largest storm in the solar system - is hundreds of degrees hotter than anywhere else on the planet. The hotspot, by process of elimination, must be heated from below, and this detection is therefore strong evidence for coupling between Jupiter's lower and upper atmospheres, likely the result of upward propagating acoustic and/or gravity waves. Our results indicate that the lower atmosphere may yet play an important role in resolving the giant planet 'energy crisis'.

On 4 December 2012 (UTC) we observed Jupiter for 9 hours using the SpeX spectrometer[8] on the NASA Infrared Telescope Facility (IRTF). The spectrometer slit was aligned along the rotational axis in the north-south direction at local noon. This arrangement is illustrated in Fig. 1**a**, which contains a slit-jaw image showing bright auroral emissions at the poles as well as a localised Great Red Spot (GRS) emission enhancement at mid-latitudes. Exposures from the instrument in this set-up give wavelength and intensity information as a function of latitude as shown in Fig. 1**b**. By exposing continuously throughout the night, we obtained longitudinal information for most of the planet (a Jovian day is 9hr 56 min).

The spectrum in Fig. 1**b** shows strong emission features at six wavelengths, which appear prominently in the auroral regions and wane towards the equator. These are discrete ro-vibrational emission lines from H_3^+, a major ion in Jupiter's ionosphere, the charged (plasma) component of the upper atmosphere. The colour contours highlight the weaker emissions from this ion across the body of the planet. Far from being a uniform intensity at low-latitudes, there is a significant intensity enhancement in all of the emission lines within the 13 - 27° planetocentric latitude range occupied by the spot[9]. As seen in the coloured contours of Fig. 1**b**, the H_3^+ emissions are isolated in wavelength, indicating that there is no continuum reflection of sunlight at red spot latitudes.

The ratio between two or more emission lines can be used to derive the temperature of the emitting ions[10,11]. With the observing geometry used here, such temperatures are altitudinally-averaged 'column temperatures' of H_3^+, where the majority of H_3^+ at Jupiter has been observed to be located between 600 to 1000 km altitude above the 1-bar pressure level[12]. H_3^+ has been demonstrated to be in quasi-local thermodynamic equilibrium throughout the majority of Jupiter's upper atmosphere, meaning that derived temperatures are representative of the co-located ionosphere and (the mostly H_2)

thermosphere[13]. In the Methods section we detail the data reduction techniques and temperature model fitting procedures, and in Fig. 2 we show two example model fits; only the strongest, outermost lines are used to fit temperatures, as the central H_3^+ lines are contaminated by telluric absorption. Note that, even though the H_3^+ peak intensities at the spot (Fig. 2, left) are lower than those at 45° latitude, this is a result of lower column-integrated H_3^+ densities at lower latitude. Derived temperatures remain unaffected by the density differences as they are based entirely on H_3^+ line ratios.

The difficulty in explaining the observed upper-atmospheric temperatures at the giant planets was realised more than 40 years ago[1], and has since been termed the giant planet 'energy crisis'[2,4]. At Jupiter, only the observed temperatures within the auroral regions have been adequately explained, as the 1000 - 1400 K temperatures[14] observed there result from auroral heating mechanisms that impart 200 GW of power per hemisphere through ion-neutral collisions and Joule heating[15,16]. The low- to mid-latitudes do not have such a heat source, and yet are measured to be near 800 K, which is 600 K warmer than can be accounted for by solar heating[15,17]. If heating does not come from above (solar heating), and cannot be produced in situ via magnetospheric interactions, then a solution is likely to be found below. Gravity waves, generated in the lower atmosphere and breaking in the thermosphere, represent a potentially viable source of upper-atmospheric heating. Previous modelling studies, however, have led to inconclusive results at Jupiter: while viscous dissipation of gravity waves in Jupiter's upper atmosphere can lead to warming on the order of 10 K, sensible heat flux divergence can also lead to cooling by a similar amount, depending on the properties of the wave[6,7]. Recent re-analysis of Galileo Probe data has shown that gravity waves impart a negligible amount of heating vertically to the stratosphere (gravity wave motion is primarily longitudinal/latitudinal) and that heating near the thermosphere is less than 1 K per Jovian day[18]. A more likely energy source is acoustic waves that heat from below (also via viscous dissipation); this form of heating requires vertical propagation of disturbances in the low-altitude atmosphere. Acoustic waves are produced above thunderstorms, and the subsequent waves have been modelled to heat the upper atmosphere by 10 K per day[19] and observed to heat the thermosphere over the Andes mountains[19,20]. At Jupiter, acoustic wave heating has been modelled to potentially impart hundreds of degrees of heating to the upper atmosphere[21]. However, to date and to the best of our knowledge, no such coupling between the lower and upper atmosphere has ever been directly observed at the outer planets, so vertical coupling has not been seriously considered as a solution to the giant planet energy crisis.

Jupiter's red spot is the largest storm in the solar system, spanning 22,000 by 12,000 km in longitude and latitude, respectively. The spot lies within the troposphere, with cloud tops reaching altitudes of 50 km, around 800 km below the H_3^+ layer[9]. Here we show in Fig. 3. (as red circles) that the pattern of H_3^+ intensity seen above the spot, when fitted to our model, gives column averaged H_3^+ temperatures of over 1600 K, higher than anywhere else on the planet, even in the auroral region. We also fitted temperatures to a swath of longitudes away from the spot in order to illustrate that the enhancement in temperature only occurs within this longitude band. The latitudinal variation of temperatures away from the spot is similar to the ranges previously observed[17], indicating that the high temperature above the spot is highly localised in both latitude and longitude.

The high temperature in the northern part of the spot provides direct observational evidence of a localised heating process. We interpret the cause of this heating to be

storm-enhanced atmospheric turbulence, which arises due to the flow-shear between the storm and surrounding atmosphere. A portion of these waves must then propagate vertically upwards, depositing their energy as heat through viscous dissipation. It is unknown, at present, why the two red data points at GRS latitudes (grey shaded region in Fig. 3) differ by 800 K. A possible observational reason could be contamination the H_3^+ line at 3.45 μm by methane emission line at the same wavelength. Any additional intensity added to this H_3^+ line results in a lower temperature (for further detail see the Methods section). Thus, the southern red spot temperature may be much higher than derived, but only if methane is preferentially brighter in the south. However, as the H_3^+ and CH_4 lines at 3.54 micron are not separated spectrally in this work, it is not possible to conclude whether or not contamination is present. An alternative physical explanation may relate to the relative velocities between the zonal wind and the spot being greatest on the equatorward side of the storm: relative velocities are 75 m/s in the north, 15 m/s in the storm core, and 25 m/s at the poleward edge[9]. The largest relative velocities would induce the strongest flow shear, leading to the greatest turbulence and therefore the largest contribution to heating above. It is possible that some signature of such a lower-to-upper atmosphere energy transfer would be deposited en route in the intervening troposphere and upper-stratosphere (0 - 150 km altitude, respectively), as there is a 10 K temperature enhancement encircling the spot at these altitudes[22,23]. However, these enhancements could also be due to the upwelling of material in the center of the storm, followed by increased adiabatic heating when the material downwells around the edges[23].

The only previous map of Jovian H_3^+ temperatures that contains the spot was made using ground-based data in 1993[17]. The authors of that study did not mention the GRS, as no obvious signature was present in their temperature map. However, based on their contours and the expected red spot location at the time, we estimate that there was a measured temperature enhancement of 50 K above the spot. While such a minor temperature increase may indicate that the GRS-driven heating of Jupiter's upper atmosphere is transient in nature, the spatial resolution of the 1993 observations was 9800 km per pixel (at the equator), compared with 500 km per pixel in this study. Thus the previous data had significantly cruder resolution in latitude and longitude. The high temperature region above the spot is localised in latitude in the present work, indicating a large temperature gradient and perhaps a confinement by presently unknown upper-atmospheric dynamics. If wave heating driven from below is responsible for the observed temperatures in Jupiter's non-auroral upper atmosphere, then we might expect a relatively smooth temperature profile with latitude, punctuated by temperature enhancements above active storms. The red spot may then simply be the 'smoking gun' that dramatically demonstrates this atmospheric coupling process, and provides the clue to solving the giant planet energy crisis.

References

1. Strobel, D. F. & Smith, G. R. On the temperature of the Jovian thermosphere. *J. Atmos. Sci.* **30**, 718-725 (1973).

2. Miller, S., Aylward, A. & Millward, G. Giant Planet Ionospheres and Thermospheres: The Importance of Ion-Neutral Coupling. *Space Sci. Series of ISSI* **116**, 319-343 (2005).

3. Smith, C. G. A., Aylward, A. D., Millward, G. H., Miller, S. & Moore, L. E. An unexpected cooling effect in Saturn's upper atmosphere. *Nature* **445**, 399-401 (2007).

4. Yates, J. N., Achilleos, N. & Guio, P. Response of the Jovian thermosphere to a transient pulse in solar wind pressure. *Planet. Space Sci.* **91**, 27-44 (2014).

5. Smith, C. G. A. & Aylward, A. D. Coupled rotational dynamics of Jupiter's thermosphere and magnetosphere. *Annales Geophysicae* **27**, 199-230 (2009).

6. Hickey, M. P., Walterscheid, R. L. & Schubert, G. Gravity Wave Heating and Cooling in Jupiter's Thermosphere. *Icarus* **148**, 266-281 (2000).

7. Matcheva, K. I. & Strobel, D. F. Heating of Jupiter's Thermosphere by Dissipation of Gravity Waves Due to Molecular Viscosity and Heat Conduction. *Icarus* **140**, 328-340 (1999).

8. Rayner, J. T. et al. SpeX: A Medium-Resolution 0.8-5.5 Micron Spectrograph and Imager for the NASA Infrared Telescope Facility. *Publ. Astron. Soc. Pac.* **115**, 362-382 (2003).

9. Parisi, M., Galanti, E., Finocchiaro, S., Iess, L. & Kaspi, Y. Probing the depth of Jupiter's Great Red Spot with the Juno gravity experiment. *Icarus* **267**, 232-242 (2016).

10. Melin, H., Miller, S., Stallard, T., Smith, C. & Grodent, D. Estimated energy balance in the jovian upper atmosphere during an auroral heating event. *Icarus* **181**, 256-265 (2006).

11. O'Donoghue, J. et al. Conjugate observations of Saturn's northern and southern H_3^+ aurorae. *Icarus* 229, 214-220 (2014).

12. Uno, T. et al. Vertical emissivity profiles of Jupiter's northern H_3^+ and H_2 infrared auroras observed by Subaru/IRCS. *J. Geophys. Res.* **119**, 10,219-10,241 (2014).

13. Miller, S., Stallard, T., Smith, C. & et al. H_3^+: the driver of giant planet atmospheres. *Phil. Trans. Roy. Soc. London.* **364**, 3121-3137 (2006).

14. Lystrup, M. B., Miller, S., Dello Russo, N., Vervack, R. J., Jr. & Stallard, T. First Vertical Ion Density Profile in Jupiter's Auroral Atmosphere: Direct Observations using the Keck II Telescope. *Astrophys. J.* **677**, 790-797 (2008).

15. Yelle, R. V. & Miller, S. Jupiter's thermosphere and ionosphere, 185-218 (Cambridge University Press, 2004).

16. Cowley, S. W. H. et al. A simple axisymmetric model of magnetosphere-ionosphere coupling currents in Jupiter's polar ionosphere. *J. Geophys. Res.* **110**, 11209 (2005).

17. Lam, H. A. et al. A Baseline Spectroscopic Study of the Infrared Auroras of Jupiter. *Icarus* **127**, 379-393 (1997).

18. Watkins, C. & Cho, J. Y.-K. The vertical structure of Jupiter's equatorial zonal wind above the cloud deck, derived using mesoscale gravity waves. *Geophys. Res. Lett.* **40**, 472-476 (2013).

19. Hickey, M. P., Schubert, G. & Walterscheid, R. L. Acoustic wave heating of the thermosphere. *J. Geophys. Res.* **106**, 21543-21548 (2001).

20. Walterscheid, R. L., Schubert, G. & Brinkman, D. G. Acoustic waves in the upper mesosphere and lower thermosphere generated by deep tropical convection. *J. Geophys. Res.* **108**, 1392 (2003).

21. Schubert, G., Hickey, M. P. & Walterscheid, R. L. Heating of Jupiter's thermosphere by the dissipation of upward propagating acoustic waves. *Icarus* **163**, 398-413 (2003).

22. Flasar, F. M. et al. Thermal structure and dynamics of the Jovian atmosphere. I - The Great Red SPOT. *J. Geophys. Res.* **86**, 8759-8767 (1981).

23. Fletcher, L. N. et al. Thermal structure and composition of Jupiter's Great Red Spot from high-resolution thermal imaging. *Icarus* **208**, 306-328 (2010).

Acknowledgements

Visiting Astronomer at the Infrared Telescope Facility, which is operated by the University of Hawaii under contract NNH14CK55B with the National Aeronautics and Space Administration (NASA). We are grateful to the observing staff at IRTF and Mauna Kea Observatory for their hard work. This work was funded by NASA under Grant No. 9500303356 issued through the Planetary Astronomy Program for L.M. and J.O'D. The UK Science and Technology Facilities Council (STFC) supported this work through the Studentship Enhancement Programme (STEP) for J.O'D, and consolidated grant support for T.S.S. and H.M (ST/N000749/1). The Royal Astronomical Society partially funded travel to take the observations. We are grateful for the planetary ephemerides that were provided by the Planetary Data System.

Author contributions

J.O'D. collected, analysed and interpreted the data and wrote the paper. L.M. greatly assisted in the data reduction, analysis, interpretation and writing of the paper. T.S. helped with the analysis and interpretation of the data. H.M. assisted in the collection and reduction of data, and provided computer code necessary for the analysis of data. All authors provided comments on the manuscript.

Author information

Reprints and permissions information is available at www.nature.com/reprints. The authors declare no competing financial interests: details accompany the full-text HTML version of the paper at www.nature.com/nature. Correspondence and requests for data and information should be addressed to JO'D (jameso@bu.edu).

Figure 1. The acquisition of Jovian spectra. In **a** we show Jupiter as observed by the SpeX slit-jaw imager and L-filter (3.13 - 3.53 μm), on 4 December 2012. Bright regions at the poles result from auroral emissions; the contrast at low- and mid-latitudes has been enhanced for visibility. The vertical beige line in the middle of the image indicates the position of the spectrometer slit, which was aligned along the rotational axis. In **b** we show the co-added spectrum of seven GRS-containing exposures; dotted horizontal lines indicate the latitudinal range of the spot. Further details are given in the Methods section.

Figure 2. Model fit to observed H_3^+ intensity as a function of wavelength. **a** is produced from the data in Fig. 1**b** between -13° and -19° planetocentric latitude, while **b** corresponds to -40° and -49° latitude. The model fit to the data is shown in solid red: only the H_3^+ lines at 3.383 μm and 3.454 μm are included in the temperature derivation (see Methods for the full list). Telluric absorption, normalised to show sky contamination, is shown in grey. The derived temperatures are **a** 1644 ±161 K and **b** 900 ±42 K (standard errors). The H_3^+ model is extended to the central region (dashed red) based on the temperatures and densities of the fits. Intensity errors are 1-sigma.

Figure 3. Jovian H_3^+ temperatures versus planetocentric latitude. Column-averaged temperatures of H_3^+ shown here are each derived from model fits to the discrete H_3^+ emission lines as shown in Fig. 2. Red circles correspond to the co-add of GRS spectra between 239 - 253 degrees system III Central Meridian Longitude (CML) shown in Fig. 1**b**. The blue triangled data was derived from exposures taken between 293 - 359 and 0 - 82 degrees CML - i.e. longitudes well separated from the spot, representing the 'ordinary' background conditions based on solar heating alone. The modelled temperature of the upper atmosphere for these non-auroral regions is 203 K[1]. Uncertainties are standard error on the mean.

Methods

Additional observing details. In Fig. 1, where we show the acquisition of Jovian spectra, Jupiter's sub-Earth latitude was +3 degrees. The configuration of the SpeX instrument on the IRTF was single order with a long slit, at a spectral resolution of R = 2,500. The slit length and width used was 60 and 0.3 arc seconds, respectively, and one pixel subtended 0.15 arc seconds on the sky. In Fig. 2 the model telluric transmission spectrum is obtained from the Atmospheric TRANsmission database (ATRAN; https://atran.sofia.usra.edu) for a spectral resolution of R = 2,500. The absorption wells near H_3^+ lines in the center of the spectrum in Fig. 2 serve to highlight our reasons for avoiding that region in the temperature fitting. The attenuation of the signal in this figure by the sky is constant as a function of latitude because all of the temperature fits are from the same exposure, so any attenuation would affect each temperature as a function of latitude in the same way.

Absolute calibration. We flux calibrated the data by using the photometric-standard A0V star HR1019 in the usual manner: i.e., by assuming a blackbody curve for the temperature of the star (10,000 K - in this case) and comparing it to what we observed. This is dual-purpose in that by dividing the data by the flux calibration, it converts counts into physical units of flux and also yields a profile of what the sky has absorbed. The mean uncertainty in the absolute calibration as a function of wavelength is 4% of the flux, and the S/N for the star was 24.

Instrumental effects. These are accounted for by flat fielding, dark-current subtraction and hot pixel removal in every frame. The calibrated Jovian spectra (containing uncertainties in absolute calibration above) also include noise from the instrumentation and Earth's atmospheric attenuation. The uncertainties are thus found by finding the standard deviation of the backgrounds in the final spectrum. All errors are propagated through with the absolute calibration and uncertainty to produce the error bars in intensity displayed in Fig. 2 and the temperature estimates in Fig. 3.

H_3^+ fitting. In order to find the temperatures from Fig. 1**b**, we used a spectroscopic H_3^+ line list[24] and the most recent H_3^+ partition function coefficients[25]. The spectrum of H_3^+ can be treated as a sum of Gaussian distribution curves, with each curve a function of temperature. This 'equation of a spectrum' is solved in order to derive the temperature[26]. This technique has been used to derive H_3^+ temperatures at Jupiter, Saturn, and Uranus for decades[27], with typical uncertainties of 10%. The fitting routines used are the same as those in previous literature[26], and include a list of over 3 million ro-vibrational transition lines of H_3^+[24]. The fitting routine uses the most recent partition function constants to establish a temperature, which are applicable for temperatures between 100 and 10,000 K (whereupon the ion dissociates)[25].

Handling of non-H_3^+ intensity. We now address the possibility of attenuation of H_3^+ by other sources at Jupiter. Possibility 1 is that there is enhanced reflection of sunlight from haze at the red spot location, but this is not seen adjacent in wavelength to any lines in Fig. 1 and can consequently be ruled out. Possibility 2 pertains to emission from neutral gases. Only the two intensity peaks overlain with solid red lines are included in the final fit, though the left peak contained the H_3 lines at 3.38285 μm and 3.38391 μm, whereas the right peak line included 3.45502 μm, 3.45483 μm and 3.45468 μm. Methane (CH4), the dominant hydrocarbon in Jupiter's atmosphere, is known to emit at a number of

wavelengths in this region, namely 3.380 μm, 3.392 μm, 3.404 μm, 3.415 μm, 3.440 μm and 3.454 μm. Some of these are visible in Fig. 1 (e.g. 3.404 μm) and some are not (e.g. 3.380 μm), but we are mainly interested in any that could affect the fitted H_3^+, which means ignoring for now the central portion of Fig. 2. The CH_4 emission line at 3.454 μm is the only line that could possibly fall on a fitted H_3^+ line, and the effect of it doing so would mean that the line ratio between the H_3^+ lines denoted by solid-red fit would be larger. For this particular set of lines, if the ratio is increased, then the temperature estimate decreases: this can be seen by comparing the ratios of lines in Fig. 2, with the lower ratio GRS spectrum corresponding to 1644 K ±161 K, while the higher ratio non-GRS spectrum is fitted as 900 ±42 K (s.e.m). In other words, if methane was contributing emission to this line, then accounting for it in some way by removing an arbitrary amount would result in the GRS temperature fitted being even higher than the 1600 K derived here.

Code availability. The H_3^+ spectroscopic line list used in the model is available online at www.exomol.com/data/molecules, in addition, an online H_3^+ intensity calculator is available at http://h3plus.uiuc.edu. The model fitting routines and reduction code used in this work is available on request (jameso@bu.edu). Our data reduction pipeline makes substantial use of the NASA Astronomy IDL library, available online at http://idlastro.gsfc.nasa.gov.

Additional references

24. Neale, L., Miller, S. & Tennyson, J. Spectroscopic Properties of the H_3^+ Molecule: A New Calculated Line List. *Astrophys. J.* **464**, 516-520 (1996).

25. Miller, S., Stallard, T., Melin, H. & Tennyson, J. H_3^+ cooling in planetary atmospheres. *Faraday Discussions* **147**, 283-291 (2010).

26. Melin, H. et al. On the anticorrelation between H_3^+ temperature and density in giant planet ionospheres. *Mon. Not. R. Astron. Soc.* **438**, 1611-1617 (2014).

27. Stallard, T. S. et al. Temperature changes and energy inputs in giant planet atmospheres: what we are learning from H_3^+. *Phil. Trans. Roy. Soc.* **370**, 5213-5224 (2012).

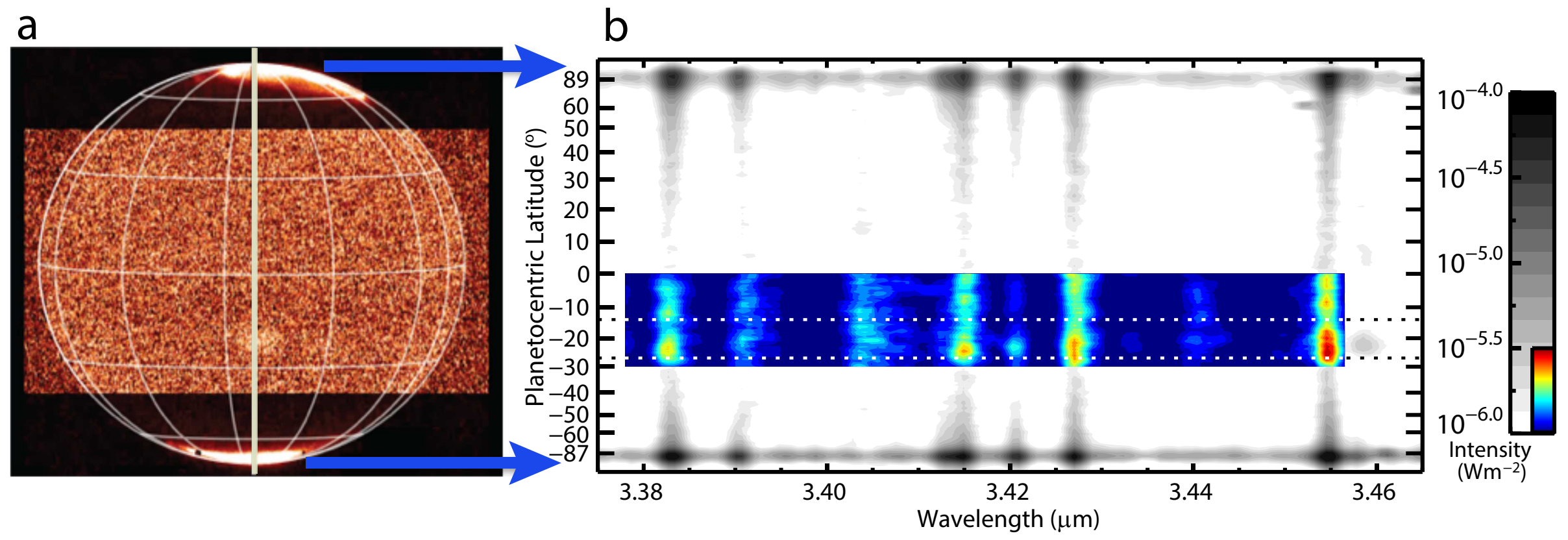
a
b
89
60
50
40
30
20
10
0
−10
−20
−30
−40
−50
−60
−87
Planetocentric Latitude (°)
3.38
3.40
3.42
3.44
3.46
Wavelength (μm)
$10^{-4.0}$
$10^{-4.5}$
$10^{-5.0}$
$10^{-5.5}$
$10^{-6.0}$
Intensity
(Wm^{-2})

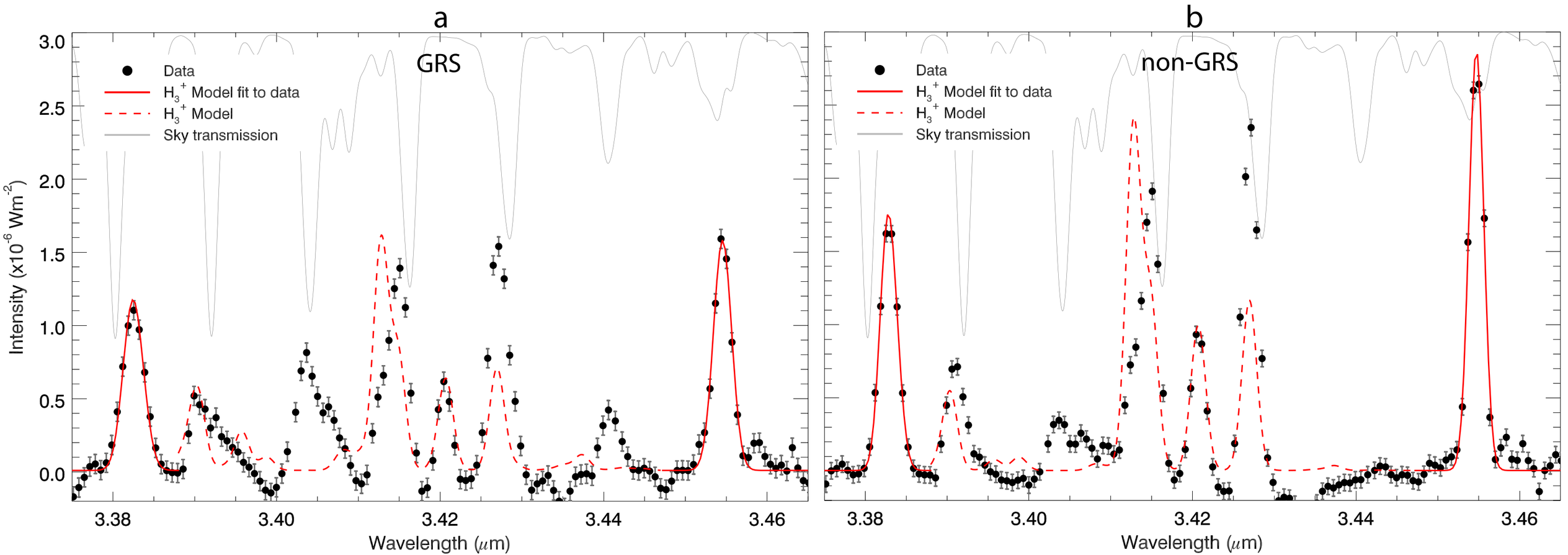
a
GRS
b
non-GRS
Data
H3+ Model fit to data
H3+ Model
Sky transmission
Intensity (x10-6 Wm-2)
Wavelength (μm)
3.0
2.5
2.0
1.5
1.0
0.5
0.0
3.38
3.40
3.42
3.44
3.46

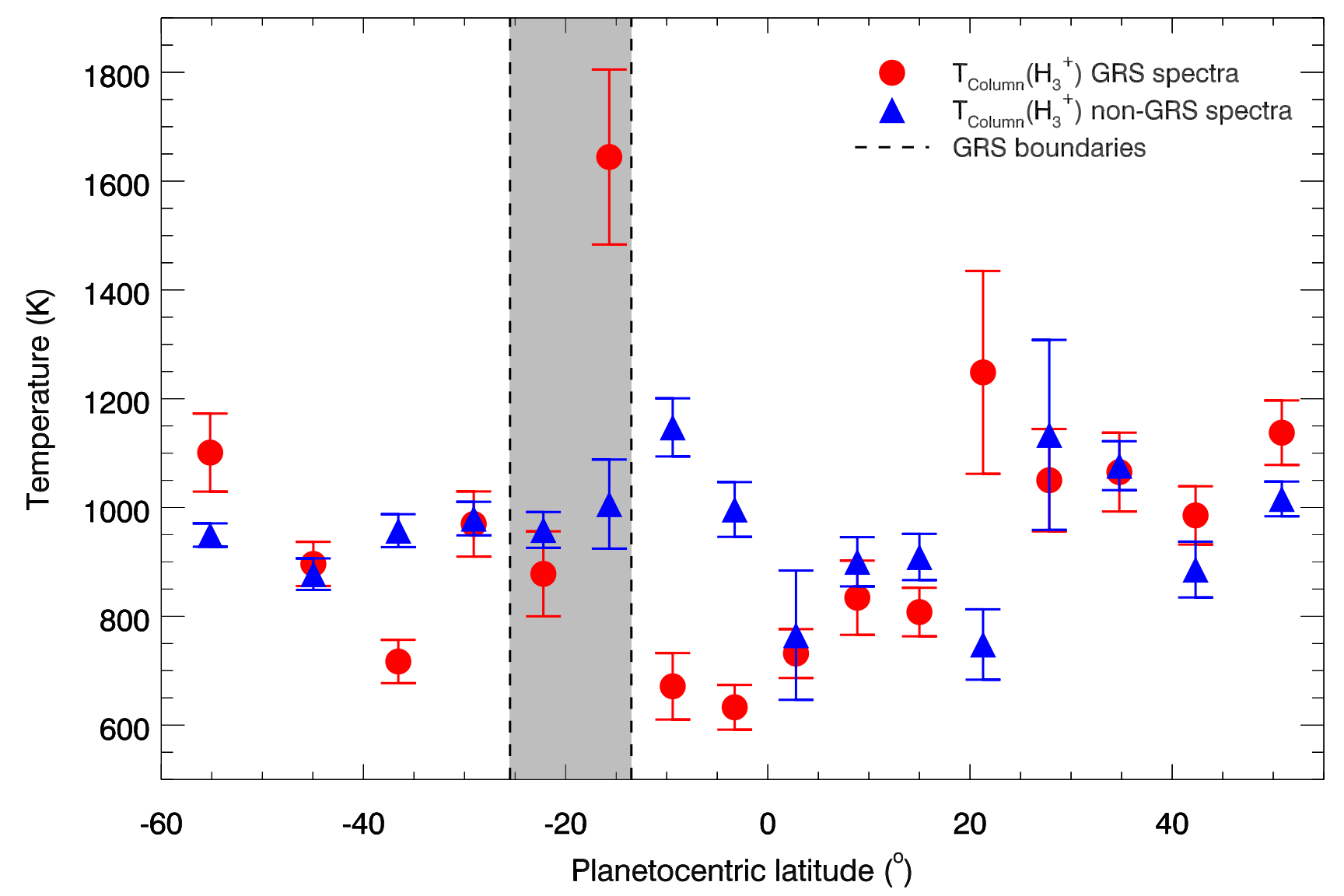
1800
1600
1400
1200
1000
800
600
Temperature (K)
-60
-40
-20
0
20
40
Planetocentric latitude (°)
T_Column(H_3^+) GRS spectra
T_Column(H_3^+) non-GRS spectra
GRS boundaries